ISSN 1062-8738, Bulletin of the Russian Academy of Sciences: Physics, 2017, Vol. 81, No. 9, pp. 1141–1145. © Allerton Press, Inc., 2017.
Original Russian Text © N.V. Popov, A.S. Mysovsky, N.G. Chuklina, E.A. Radzhabov, 2017, published in Izvestiya Rossiiskoi Akademii Nauk, Seriya Fizicheskaya, 2017, Vol. 81, No. 9, pp. 1269–1273.

Theoretical Study of Divalent Samarium Defects in Lanthanum Fluoride Crystals

N. V. Popov[a, b, *], A. S. Mysovsky[a, b], N. G. Chuklina[a, b], and E. A. Radzhabov[a]

[a] *Vinogradov Institute of Geochemistry, Siberian Branch, Russian Academy of Sciences, Irkutsk, 664033 Russia*

[b] *Irkutsk National Research Technical University, Irkutsk, 664074 Russia*

**e-mail: brodiaga38@gmail.com*

Abstract—The results from a theoretical study of the electron structure of an impurity rare-earth Sm^{2+} defect in a LaF_3 crystal are presented. The electron energy levels of the rare-earth impurity defect and the transitions between them are studied using the multiconfigurational CASSCF/CASPT2 method. The absorption spectrum obtained during the calculations is consistent with the experimental data. Based on our model, we can state definitively that a vacancy on an anion sublattice serves as a charge compensator for a divalent ion.

DOI: 10.3103/S1062873817090192

INTRODUCTION

The electronic structure of rare-earth trivalent defects in lanthanum fluoride crystals has been studied in detail by theoretical and experimental means [1–3]. Divalent rare-earth ions in a lanthanum fluoride crystal have been studied much less. The slight greenish color of some grown crystals of LaF_3-SmF_3 was associated with the transformation of a small portion of Sm^{3+} into Sm^{2+} [4]. The formation of Sm^{2+}defects is possible in LaF_3 if such divalent centers are present in the LaF3-related crystals: $LaCl_3$ and $LaBr_3$ [5]. Since Sm^{2+} replaces trivalent atoms in a cation sublattice, we may assume that the anion vacancy nearest to a defect acts as a charge compensator.

The authors of [6] experimentally studied the optical spectra and electrical conductivity of LaF_3 crystals activated by Sm^{2+} ions. It was shown that several bands in a glow spectrum of 560–620 nm, 650–690 nm, and 680–770 nm, measured at a temperature of 7.9 K, were caused by transitions from $^5D_2$, $^5D_1$, and $^5D_0$ to the ^7F_j levels of a Sm^{2+} ion. The existence of an anion vacancy was proved by the linear dependence of the electrical ionic conductivity of crystals on the value of Sm^{2+} absorption bands associated with the movement of vacancies. The optical absorption spectrum presented in this work contains a long-wave band at 600 nm that is missing from in the excitation spectra. We interpret it as a transition from the ground state of a rare-earth defect to the 1*s*-level of the vacancy.

It was established in [7] that a vacancy creates levels in the forbidden zone of a crystal. A transition to the level of the vacancy in this system means the capture of an electron by a vacancy, followed by the formation of an *F*-center. A vacancy that captures an electron this way behaves as a hydrogen-like atom; its ground state into which an electron transforms from a rare-earth defect is described by hydrogen-like wave functions.

The aim of this work was to model the electronic structure of a Sm^{2+}-vacancy system in a LaF_3 crystal.

MODELING

We made a series of quantum-chemical calculations to confirm the hypothesis regarding the nature of a charge compensator from [6]. They can be conventionally divided into two parts: calculations of the structure (geometry) and precise calculations of the energy level of a defect. Calculating the geometry means searching for structural parameters of the system that could ensure the local minimum of the total energy of the system.

The geometry was calculated in two ways: using a quantum cluster in the nonperiodic approximation and using the density functional theory for periodical systems. We used two different ways of calculating the geometry of a defect and the mechanism of charge compensation for a number of reasons: the defect environment must be polarized in the same direction no matter which method we use; only differences in the displacement amplitudes are allowed. We performed precise calculations of the energy levels for the obtained defect structure by multiconfigurational methods with respect to dynamic correlation and relativistic corrections.

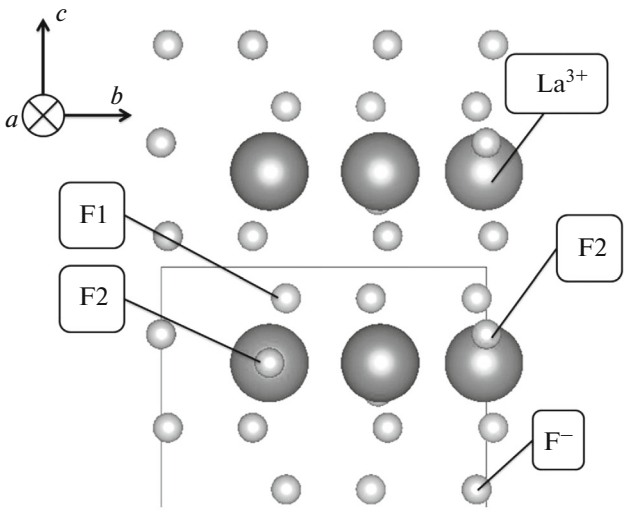

Fig. 1. Position of fluorine nodes in our LaF_3 crystal (crystal axis *a* is directed toward the reader) with a tysonite structure: F1, between the planes; F2, in the plane with lanthanum; F3, same as F2, but shifted along axis *c*.

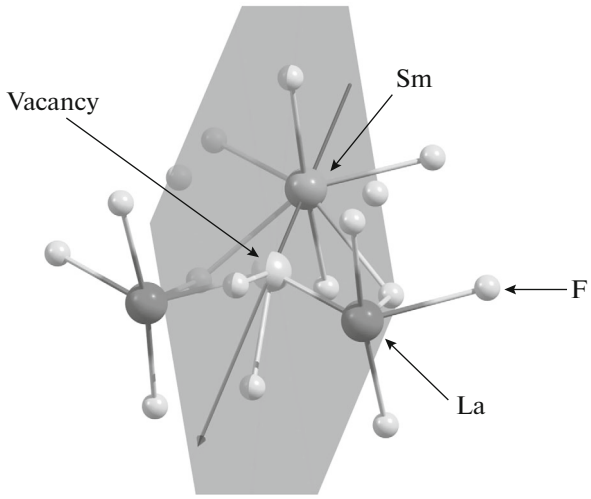

Fig. 2. Quantum cluster $SmLa_2F_{13}$ with C_{2v} symmetry. The corresponding second order axis of rotation and the vertical plane of reflection are shown.

NATURE OF A CHARGE COMPENSATOR

A charge compensator is needed to preserve the electrical neutrality of a LaF_3 crystal when a Sm^{2+} defect forms in the cation sublattice of a LaF_3 crystal. The easiest possible way of doing this is to form vacancies in the F-sublattice. Vacancies can have several positions in the anion sublattice with respect to the spatial group of a LaF_3 crystal (Fig. 1). Three unique positions of fluorine are recognized for a tysonite structure: between the lanthanum planes (F1), in the plane with lanthanum (F2), and fluorine shifted slightly from the plane with lanthanum (F3). In the hexagonal syngony, F2 and F3 are equivalent. In this work, we consider only the structure of tysonite.

Quantum Clusters

In this method, we split our model into several regions described in different ways: a quantum cluster described in a quantum-chemical way; an interface region described using pseudopotentials; and a classical region described by classical pair potentials. This approach enables us to model the local environment for an impurity defect with respect to polarization of the environment. We tested this method in calculations for intrinsic and impurity defects in fluoride crystals [7, 8].

To optimize the defect structure, we used a $SmLa_{12}F_{40}$ quantum cluster. A diffuse double-exponential basis set was used for all atoms in the cluster: Sm [9], La [10], and F [11]. For the interface atoms, we used pseudopotentials La and F [12]. The calculations were performed using the PC Gamess Firefly software package [13].

Density Functional Theory for Periodic Systems

We used supercell method to model point defects: a reduced or a unit cell of a lattice was repeated along its translation vectors a particular number of times. We thus obtained a new enlarged cell with a new crystal basis. To model the simplest point vacancy, we construct a super cell from the base cells of a crystal, one of which will have a defect. It is important in this case to verify the convergence of the system and ensure the image of a defective cell has no effect on the modeled defect itself.

To model the Sm^{2+}-anion vacancy system, we constructed a super cell of $3 \times 3 \times 2$, which consisted of 143 atoms (36 lanthanum atoms and 107 fluorine atoms). Our calculations were performed in the local density approximation [14] using the PBE functional [15] in the VASP software [16] and an embedded set of standard pseudopotentials.

Modeling a Charge Compensator

Our calculation results showed that the F2 vacancy is more energy advantageous than the F1 vacancy (by 0.25 eV) and the F3 vacancy (by 0.44 eV), according to the results from quantum-cluster modeling. It was more energy advantageous than the F1 vacancy (by 0.35 eV) and the F3 vacancy (by 0.55 eV) when we used the theory of density functional in the periodical approximation. Both methods showed the same direction of the shift of the nearest atoms around a vacancy; only the shift amplitudes were different. The average difference between the two types of calculations was 0.25 Å. Figure 2 shows symmetry C_{2v} of the defect obtained by analyzing the structural parameters of the immediate environment.

The ground electronic state of a rare-earth defect was $4f^6$ in both cases with multiplicity $S = 7$, which is the maximum for this number of electrons. We also found that states with different multiplicities initially have greater energy, but their geometry was not optimized.

MODELING EXCITED STATES OF A RARE-EARTH DEFECT

Our calculations for excited electronic states performed using the CASSCF (Complete Active Space Self Consistent Field) method [17] with averaging over the states in the Molcas software [18]. Using a large $SmLa_{12}F_{40}$ cluster to optimize the geometry, we identified a smaller cluster of $SmLa_2F_{14}$.

To describe the electronic structure of the vacancy, we added a 1*s*-basis function to the place of its possible localization. This was needed to avoid extending the 1*s*-levels of the vacancy from the 5*d*-functions of $Sm^{2+}$and La^{3+} surrounding a La^{3+} vacancy.

The correlation corrections were considered using the CASPT2 (Complete Active Space Second Order Perturbation Theory) method [19]. The spin-orbit states were constructed on the basis of spin-free states using the one-electron Hamiltonian of spin-orbit interaction according to the interaction between restrictive active space states [20] (RASSI, Restrictive Active Space State Interaction). This technique allows us to calculate the matrix elements of operators between different representations of a multi-electron wave function, but not only in the representation of a restrictive active space.

Sm [21], La [21], and F [22] were used as the basis of the atoms in the quantum cluster; La [23] and F [24] were used as pseudopotentials on the interface atoms.

Energy Levels

We estimated the excited states of Sm^{2+} from the calculated geometry of a defect and its environment. The ground state of a rare-earth defect in multiconfigurational calculations is ^7F. Note that due to the character of the effect the type of vacancy has on the structure of Sm^{2+} levels they can be considered equivalent; i.e., the energy spectrum of the lowest $4f^6$-states does not change strongly (on the order of ~10 cm^{-1} only) with respect to the node of vacancy localization.

Averaging was performed separately for the following groups of states: $4f^6$ (6 electrons on the 4*f*-orbitals of samarium), $4f^5V^1$ (5 electrons on the 4*f*-orbitals of samarium and 1 electron on the vacancy orbital), and $4f^55d^1$ (5 electrons on the 4*f*-orbitals of samarium and 1 electron on 5*d*).

Our initial study included the lowest $4f^6$-states of all possible values of this system's multiplicity: 7, 5, 3, and 1. Calculations revealed that states with different multiplicities do not mix, and states with multiplicities 3 and 1 lie much higher with respect to the energy than those with multiplicities 7 and 5. Accurate averaging followed by calculating correlation corrections and the transition to the spin-orbital states were thus performed using the $4f^6$ ^7F- and ^5D-states.

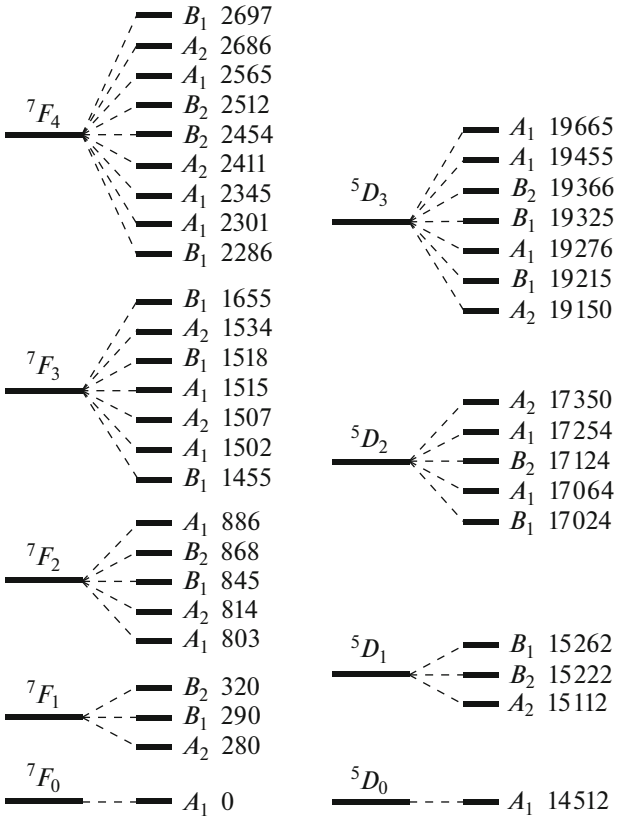

Fig. 3. Diagram of the lowest of the $4f^6Sm^{2+}$-states, with energy expressed in cm^{-1}.

To characterize the states that belong to the C_{2v} symmetry group so long as the number of electrons was even, we used the direction of polarization of the dipole moment of the transition between the states.

A diagram of the lowest $4f^6$-states is presented in Fig. 3. The ground state for this defect is $^7F_0$; the next group, $^7F_1$, is higher than the ground state by 300 cm^{-1}; the $^7F_2$ group, by 800 cm^{-1}; the $^7F_3$ group, by 1400 cm^{-1}; and the $^7F_4$ group, by 2200 cm^{-1}. The states inside the groups were split along the projection of the total momentum: $^7F_0$, 1; $^7F_2$, 3; $^7F_3$, 5; $^7F_4$, 7. The lowest state with multiplicity 5 is $^5D_0$, and it is higher than $^7F_0$ by 17000 cm^{-1}; the next group of excited states with this multiplicity, $^5D_1$, is higher than $^7F_0$ by 19000 cm^{-1}; and $^5D_2$ is higher by 21000 cm^{-1}. The lowest states inside the group, $S = 5$, were also split along the projection of the total momentum: $^5D_0$—1; $^5D_1$—3; and $^5D_3$—5. This pattern is consistent with the experi-

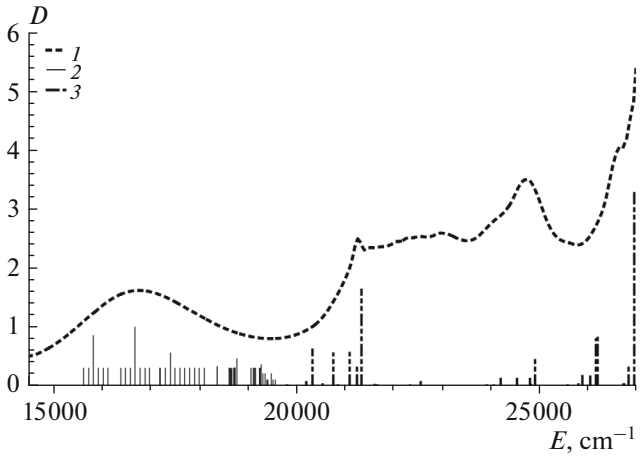

Fig. 4. Absorption spectrum of Sm^{2+} in a LaF_3 crystal. The plot represents three datasets: (*1*) the experimental absorption spectrum in [6] (dashed line); (*2*) the calculated transitions from $4f^6Sm^{2+}$to the $4f^5$ + vacancy (vertical lines); and (*3*) the calculated transitions from $4f^6$ Sm^{2+} to $4f^55d^1$ (dashed vertical lines).

mental luminescence spectra of Sm^{2+}:LaF_3. The $4f^6$-levels of Sm^{2+} changed slightly in crystals with the ReX_3 structure ($LaCl_3$, $LaBr_3$) and had the same character of the splitting of states and the energy in crystals of this type [5].

The obtained states of the rare-earth ion and vacancy are conveniently represented as a combination of an atomic term Sm^{3+} and the ground level of a vacancy, which we denote as *V*. The electron configuration of this system can be presented as a combination of the ion term and the level of a vacancy. The lowest state for system $4f^5V^1$ with respect to the energy is thus $\left|{}^6H_{5/2},V^1\right\rangle$ According to the results from modeling, we obtained five groups of such levels in the energy range of 15500–18000 cm^{-1}: $\left|{}^6H_{5/2},V^1\right\rangle$, $\left|{}^6H_{7/2},V^1\right\rangle$, $\left|{}^6H_{9/2},V^1\right\rangle$, $\left|{}^6H_{11/2},V^1\right\rangle$, and $\left|{}^6H_{13/2},V^1\right\rangle$. There were 6, 8, 10, 12, and 14 levels in these groups. A broadened band was observed in the above range of the energy in the experimental spectrum of absorption. This band can be obtained if the density of the levels is high at the given range of energy. If spin–orbit interaction $\left|{}^6H_{5/2},V^1\right\rangle$ is not considered, the energy of the state is 13100 cm^{-1}. If spin–orbit corrections are considered, there is splitting between states $\left|{}^6H_{5/2},V^1\right\rangle$ and $\left|{}^6H_{7/2},V^1\right\rangle$, which shifts the states of group $\left|{}^6H_{5/2},V^1\right\rangle$ with respect to energy by 2000 cm^{-1} and $\left|{}^6H_{7/2},V^1\right\rangle$ by 1000 cm^{-1}. The energies of the other states do not change much when spin–orbit corrections are considered (~100 cm^{-1}), and the states are merely split.

We calculated the electronic structure of the $4f^55d^1$-levels. According to our calculations, the groups of these levels lie in the range of 20000–32000 cm^{-1}. These levels are hard to compare to the experimental absorption spectrum, due to the vibronic-broadened lines in this region. However, we can say that these states are higher with respect to energy than the $4f^5$:vacancy states.

The intensities of the transitions from the ground state to a vacancy are comparable to the calculated intensities of the transitions to the lowest $4f^55d^1$-states, which is confirmed by the experimental data. The oscillator strength of the calculated transitions between ${}^7F_0$-${}^7F_j$ and ${}^7F_0$-${}^5D_j$ was four orders of magnitude lower than the transitions from the ground state to the vacancy and $4f^6 \rightarrow 4f^55d^1$, so they are not seen in the experimental spectrum of absorption. Figure 4 compares the calculated absorption spectrum and the experimental data and shows the good agreement between the calculated and experimental data.

CONCLUSIONS

We obtained a model for the electronic structure of Sm^{2+} centres in a LaF_3 crystal via quantum-chemical calculations using the embedded cluster approximation. To ensure the electrical neutrality of the crystal, the anion vacancy acted as a charge compensator for this defect. The symmetry obtained for these centers was C_{2v}. The broadened band in the absorption spectrum was a transition from the ground ${}^7F_0$ $4f^6$ state of samarium to the levels of the vacancy with the formation of an *F*-center.

ACKNOWLEDGMENTS

Our calculations were performed using the resources of the Academician V.M. Matrosov computing cluster at the Institute for System Dynamics and Control Theory, Siberian Branch, Russian Academy of Sciences [25], and the Information Computer Center of Novosibirsk State University [26].

REFERENCES

1. Rast, H.E., Fry, J.L., and Caspers, H.H., *J. Chem. Phys.*, 1967, vol. 46, no. 4, p. 1460.
2. Neogy, D. and Purohit, T., *Phys. Status Solidi (b)*, 1987, vol. 139, no. 2, p. 519.
3. Carnall, W.T., et al., *J. Chem. Phys.*, 1989, vol. 90, no. 7, p. 3443.
4. Weller, P.F. and Kucza, J.A., *J. Appl. Phys.*, 1964, vol. 35, no. 6, p. 1945.
5. Dieke, G.H., et al., *Spectra and Energy Levels of Rare Earth Ions in Crystals*, New York: Interscience, 1968.

6. Radzhabov, E.A. and Kozlovsky, V.A., *Phys. Procedia*, 2015, vol. 76, p. 47.
7. Mysovsky, A.S., et al., *Phys. Rev. B*, 2011, vol. 84, no. 6, p. 064133.
8. Popov, N., et al., *Radiat. Meas.*, 2016, vol. 90, p. 55.
9. Pantazis, D.A. and Neese, F., *J. Chem. Theory Comput.*, 2009, vol. 5, no. 9, p. 2229.
10. Neto, A.C. and Jorge, F.E., *Chem. Phys. Lett.*, 2013, vol. 582, p. 158.
11. Neto, A.C., et al., *J. Mol. Struct.: THEOCHEM*, 2005, vol. 718, no. 1, p. 219.
12. Hay, P.J. and Wadt, W.R., *J. Chem. Phys.*, 1985, vol. 82, no. 1, p. 270.
13. http://classic.chem.msu.su/gran/firefly/index.html.
14. Kohn, W. and Sham, L.J., *Phys. Rev.*, 1965, vol. 140, no. 4A, p. A1133.
15. Perdew, J.P. and Zunger, A., *Phys. Rev. B*, 1981, vol. 23, no. 10, p. 5048.
16. Kresse, G. and Furthmüller, J., *Comput. Mater. Sci.*, 1996, vol. 6, no. 1, p. 15.
17. Roos, B.O., et al., *Chem. Phys.*, 1980, vol. 48, no. 2, p. 157.
18. Karlstrom, G., et al., *Comput. Mater. Sci.*, 2003, vol. 28, no. 2, p. 222.
19. Finley, J., et al., *Chem. Phys. Lett.*, 1998, vol. 288, no. 2, p. 299.
20. Malmqvist, P., Roos, B.O., and Schimmelpfennig, B., *Chem. Phys. Lett.*, 2002, vol. 357, no. 3, p. 230.
21. Roos, B.O., et al., *J. Phys. Chem. A*, 2008, vol. 112, no. 45, p. 11431.
22. Roos, B.O., et al., *J. Phys. Chem. A*, 2004, vol. 108, no. 15, p. 2851.
23. Sadoc, A., Broer, R., and de Graaf, C., *J. Chem. Phys.*, 2007, vol. 126, no. 13, p. 134709.
24. Lopez-Moraza, S., Pascual, J.L., and Barandiaran, Z., *J. Chem. Phys.*, 1995, vol. 103, no. 6, p. 2117.
25. http://hpc.icc.ru.
26. http://clu.nusc.ru.

Translated by L.V. Mukhortova